Monte Carlo study of the collapse transition of flexible and semiflexible star-branched polymers

Andrzej Sikorski
Department of Chemistry, University of Warsaw, 02-093 Warszawa, Poland

(Received 22 October 1991; revised 1 May 1992)

Detailed results are presented of dynamic Monte Carlo simulations of the uniform star-branched polymer model confined to a diamond lattice. The model macromolecule consists of $f=4$ arms, every arm of identical length in the range of 11 to 199 statistical segments. The model incorporates interaction between the nearest neighbour segments and local stiffness (a preference of the *trans* states over both *gauche* states). The size and shape of a polymer chain was studied for various solvent conditions and various degrees of stiffness. The appropriate scaling laws are described. The Θ conditions were also determined. Two different types of collapse transitions were found for the flexible chains and for stiff chains, similarly to the case of linear chains.

(Keywords: Monte Carlo simulation; star polymer; flexibility)

INTRODUCTION

Branched polymers have been an object of theoretical studies for many years, starting with the well known work of Zimm and Stockmayer. There are many simplified polymer topologies: stars, combs, brushes and rings. This paper examines uniform star-branched polymers, defined as structures in which linear chains of the same length emanate from a central point (branching point). The number of branches is called the functionality and is denoted by f. Recently some theoretical works were published which focused on the influence of the number of branches on size and shape of a macromolecule under various conditions[2-10] and on dynamic properties[10]. In this paper we concentrate on the influence of branching on thermodynamic properties of a single macromolecule, using $f=4$. Monte Carlo simulations of some dynamic properties of star-branched macromolecules will be presented elsewhere[11]. It should be pointed out, however, that for higher functionalities ($f>6$) the behaviour of star-branched polymers is different, especially for finite length of arms[5].

The behaviour of a single macromolecule (in an infinitely dilute solution), whether branched or linear, can be modelled by random walks on quasi-crystalline lattices[12]. For a chain with excluded volume (i.e. non-selfintersecting chain) parameters describing size and shape of a macromolecular coil obey scaling laws[12-14]:

$$\langle R_N^2\rangle = AN^\gamma \tag{1a}$$

$$\langle S_N^2\rangle = BN^\gamma \tag{1b}$$

where $\langle R_N^2\rangle$ is the mean square end-to-end distance (centre-to-end distance for star-branched polymers), $\langle S_N^2\rangle$ is the mean-square radius of gyration and N is the total number of statistical segments in a polymer chain. Parameters A and B depend on the dimension of space and on the local details (e.g. lattice). γ seems to be a universal exponent depending only on the dimensionality. In the case of athermal solution (no interactions with the sole exception of the excluded volume) or in good solvent conditions[12-14] its value is close to 6/5, which is in agreement with Flory's original theory[15]. Recently it has been calculated very precisely using simulation techniques and analytical theories for linear and for branched polymers[16-20] (see below). γ is thought to be independent of f in star polymers[2,5,7,8]. With decreasing temperature or with deteriorating solvent conditions, the size of a polymer coil diminishes and at the so-called Θ point[13,15] $\gamma=1$. Thus, in Θ conditions the size of a polymer chain is described by the same exponent γ as in the case of a random flight chain (i.e. a chain with no excluded volume) but the chain is not Gaussian[13]. Below the Θ point a polymer chain collapses. In the case of a linear chain one can distinguish two different cases of collapsed structures: (i) a dense disordered globule, where scaling theories predict exponent $\gamma=2/3$; and (ii) a dense highly ordered state[6]. The value of the Θ temperature is believed to be identical for linear chains and star-branched polymers in the limit of the infinite length of chain, although it was proved in lattice Monte Carlo simulations[21,22] that the Θ temperature decreases with increasing functionality of a star-branched macromolecule. According to small-angle neutron scattering (SANS) experiments by Huber *et al.*[23], real star-branched polymers do not exhibit Gaussian behaviour in Θ conditions.

A branched polymer chain occupies considerably smaller space compared to a linear chain with the same total number of segments. The ratio:

$$g = \langle S_N^2\rangle_{\mathrm{br}}/\langle S_N^2\rangle_{\mathrm{l}} \tag{2}$$

is a commonly used measure of the size of a branched

0032-3861/93/061271-11

polymer. Subscript br means branched and l means linear chain. For the random flight chain model, Zimm and Stockmayer[1] found:

$$g=(3f-2)/f^2 \qquad (3)$$

in the limit of the infinite length of the arm of a star. Values of parameter g obtained in computer simulations[5,7] for good solvent conditions (above the Θ temperature) are surprisingly close to those for random flight chains (equation (3)). Values of g found in experiments (at the Θ temperature) are also in agreement with the Zimm–Stockmayer formula. Not long ago Bishop and Clarke[24] (using Brownian dynamics in the continuum space) proved that star-branched macromolecules with $f=3$ arms collapse to the same structures as linear chains, i.e. to a sphere (parameter g approaches 1).

A considerable number of theoretical papers[3–10,21,22,24–41] have recently focused on star-branched polymers. Apart from star polymers, the most frequent subjects of theoretical studies are polymer combs[42,43] and brushes[43,44]. Among theoretical works on star-branched polymers there are Monte Carlo simulations of lattice models[5,7,22,27–31], off-lattice chains with Lennard–Jones type interactions[34–39], molecular dynamics simulations of stars with many arms (f up to 50)[6,40], iterative convolution approximation[33] and Brownian dynamics simulations[24,34–39]. It has recently become possible to synthesize well defined uniform stars and to study them experimentally[45–51] mainly by means of SANS and dynamic light scattering (d.l.s.). Thus, simulation results can now be related not only to analytical theories but to real experiments.

DESCRIPTION OF THE MODEL

The model is confined to a tetrahedral (diamond) lattice. The number of arms in the star polymer is limited by a lattice coordination number, z. In the case of a tetrahedral lattice, $z=4$, which implies that the maximum number of arms is $f=4$. Every arm consists of n beads located on diamond lattice sites connected with n units (segments, monomers). The $(n+1)$th point is common for every arm. On a tetrahedral lattice eight different orientations of segments are allowed: $\beta_1=[1,1,1]$, $\beta_2=[1,1,-1]$, $\beta_3=[1,-1,1]$, $\beta_4=[-1,1,1]$, $\beta_5=[-1,-1,-1]$, $\beta_6=[1,-1,-1]$, $\beta_7=[-1,1,-1]$ and $\beta_8=[-1,-1,1]$. In order to maintain a correct lattice geometry, segments in a linear chain are allowed in a certain sequence: only one coordinate changes its sign when going from β_i to β_{i+1}, e.g. only β_2, β_3 and β_4 are allowed after β_1. In order to introduce a proper volume of a macromolecule the double occupancy of lattice sites is forbidden.

The model described above corresponds to a discrete version of the rotational isomeric states (RIS) model with excluded volume. It is possible to implement a local potential very easily in order to mimic some conformational stiffness as in real polymers. Every three consecutive segments of an arm determine a conformational state: *trans* (t), *gauche* minus ($g-$) and *gauche* plus ($g+$). The rotational potential was assumed to be equal to zero for the *trans* states and to be equal to $\varepsilon_g \geqslant 0$ for both the *gauche* states. Long distance potential (long distance means that interacting segments are far along the chain contour but close in space) was introduced in a familiar way: any pair of non-bonded segments interact with the following mean force potential:

$$V_{ij}=\begin{cases}0 & \text{for } |\boldsymbol{r}_i-\boldsymbol{r}_j|>l\\ \varepsilon_a & \text{for } |\boldsymbol{r}_i-\boldsymbol{r}_j|=l\\ \infty & \text{for } |\boldsymbol{r}_i-\boldsymbol{r}_j|<l\end{cases} \qquad (4)$$

where parameter $\varepsilon_a<0$ (an attractive force), $l=|\beta_i|=3^{1/2}$ is the length of a segment and $\boldsymbol{r}_i$, $\boldsymbol{r}_j$ are coordinates of the ith and jth segments, respectively. The total configurational energy of the star-branched macromolecule E_{conf} is given by:

$$E_{\text{conf}}=\nu_a\varepsilon_a+\nu_g\varepsilon_g \qquad (5)$$

where ν_a is the number of contacts between non-bonded segments and ν_g is the number of both *gauche* states in a given configuration of a chain.

COMPUTATIONAL PROCEDURE

The choice of the Monte Carlo sampling procedure is crucial to the proper calculations of parameters of the collapse transition. The configurational space has to be sampled in a random coil state as well as in the collapsed state. The dynamic Monte Carlo (DMC) was found to be very useful in studying the collapse transition of lattice models of linear polymers and extremely useful for studying the folding transition of lattice models of globular proteins[52]. The sampling procedure is based on the asymmetric metropolis scheme[12,16,17]. The small and local modification of an 'old' conformation leads to a 'new' conformation. The new conformation is accepted with the probability:

$$P=\min[1,\exp(-\Delta E/k_B T)] \qquad (6)$$

where $\Delta E=E_{\text{new}}-E_{\text{old}}$, k_B is Boltzmann's constant and T is the absolute temperature. In the limit of a long Monte Carlo run the distribution of states approaches an equilibrium Boltzmann distribution.

The Monte Carlo step consists of the following set of local micromodifications:

(i) three-bond flip motion which changes states $g+$ ($g-$) into $g-$ ($g+$) in a randomly chosen part of the polymer chain (*Figure 1a*);
(ii) four-bond kink motion of a randomly chosen part of the polymer chain (*Figure 1b*);
(iii) a random reorientation of the two end segments of each arm (*Figure 1c*);
(iv) four-bond wave motion exchanges four consecutive bonds of a chain forming a sequence of states $g+g-$ ($g-g+$) with two bonds located elsewhere in the same arm, to preserve the length of an arm (*Figure 1d*);
(v) five-bond wave motion where five consecutive bonds of a chain forming a cyclohexane-like ring are exchanged with a single bond located elsewhere in the same arm (*Figure 1e*).

It was shown that the first three micromodifications span the entire conformational space (i.e. any allowed conformation can be achieved using this set of modifications). Micromodification (ii) is very important because it introduces new local orientations, while micromodification (i) only causes diffuse local orientation along the chain. The wave motions (iv) and (v) play the role of internal reptation moves (a regular reptation move is not

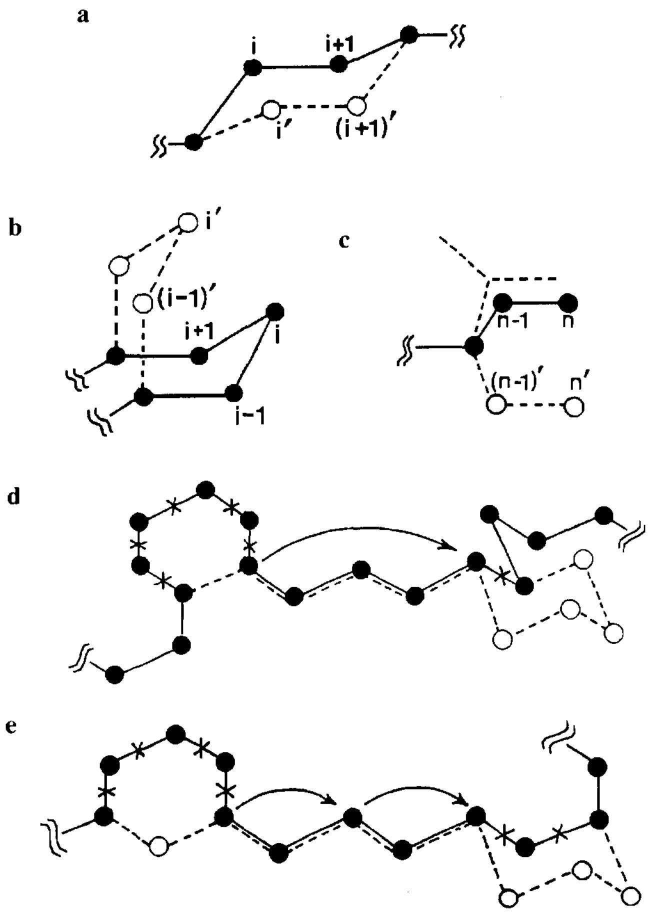

Figure 1 (a) Three-bond flip motion; (b) four-bond kink motion; (c) two-bond end rotation; (d) four-bond wave motion; (e) five-bond wave motion

used because of the condition that an arm should have a constant length). These types of moves shift local conformation along the chain and thus they are very important at lower temperatures[16,17,52,53] because they are able to unfold configurations which correspond to local (not global) energy minima. They help to reduce the number of Monte Carlo steps required to reach an equilibrium state. The time scale is distorted when wave motions are used but we are not interested in dynamic properties of the model star polymer. The frequency of particular micromodifications is basically the same as in previous works[16,17]: a time unit (Monte Carlo step) consists of f end modifications, $f(n-3)$ three-bond flip motions and $4f(n-3)$ four-bond kink motions (the factor 4 was found experimentally to be efficient). Wave motion frequency changes with temperature and with the ratio of short-range to long-range interactions. Generally it is of a lower order of magnitude than those of three-bond flip motions. It should be pointed out that the central (branching) point is not subject to these moves; it can be immobile in the case of the simulation of equilibrium properties. This behaviour of the branching point provides some technical advantages which are discussed below.

Every simulation run consists of 10^5 to 10^7 Monte Carlo steps. Of course this number depends strongly on other parameters such as temperature, ratio of interactions, etc. The metropolis criterion is applied after every single micromodification in order to accept or reject a new conformation. In order to check if the algorithm is ergodic and to ensure that an equilibrium state was reached, simulations were performed for the same set of parameters starting from a different initial configuration and using different streams of random numbers. In the collapse transition region, heating and cooling sequences were undertaken to ensure that a model macromolecule was not locked in a long-lived metastable state.

In a single DMC run after a relatively short equilibration time, averages of some parameters were calculated by collecting data every 100–1000 steps. The mean-square radius of gyration is calculated as:

$$\langle S_N^2\rangle = \frac{1}{N+1}\sum_{i=1}^{N+1}\langle(\mathbf{r}_i-\mathbf{r}_{\mathrm{cm}})^2\rangle \tag{7}$$

where the averaging $\langle\ldots\rangle$ is over the DMC steps for which the data were collected along the simulation run, $\mathbf{r}_i$, is the coordinate vector of the ith bead, $\mathbf{r}_{\mathrm{cm}}$ is the coordinate of the centre of mass and $N=fn$ is the total number of segments ($N+1$ is the number of polymer beads). This parameter describes the size and the shape of the entire polymer chain. The mean-square centre-to-end distance gives information on an average arm of the chain:

$$\langle R_N^2\rangle = \frac{1}{f}\sum_{i=1}^{f}\langle(\mathbf{r}_{ni}-\mathbf{r}_0)^2\rangle \tag{8}$$

where $\mathbf{r}_{ni}$ is the coordinate of the end of the ith arm and $\mathbf{r}_0$ is the coordinate of the branching point. The reduced fourth moment of the radius of gyration was also calculated. The average fraction of *trans* states is given by:

$$\langle f_t\rangle = \left\langle\frac{v_t}{f(n-3)}\right\rangle \tag{9}$$

where v_t is the number of *trans* states in a single conformation. The average conformational energy was calculated according to the equation (2) and averaged over many configurations. The mean-square energy was also calculated.

RESULTS

The simulations were made for star-branched polymers with $n=11$, 24, 49, 99 and 199 beads in an arm and thus for a total number of beads of 45, 97, 197, 397 and 797, respectively (the length of an arm considerably exceeds the persistence length). The model chain was placed into the Monte Carlo box with edge length $L=25$ to 200. Hence, because of the immobility of the branching point, the entire chain was always inside the Monte Carlo box with the sole exception of the case where $n=199$. This enables more extensive calculations to be made because periodic boundary conditions[12], which consume a considerable amount of computer time, were needed only for the case of $n=199$. Two different reduced temperatures T^* were defined for flexible and semiflexible polymers, respectively. In the first case $T^*=k_BT/\varepsilon_a$ (the only energetic parameter in this model) and in the second case $T^*=k_BT/\varepsilon_g$ (based on local interactions). All the DMC simulations were performed on IBM PC-386 computers and on a SUN SPARC 2 computer in the Department of Chemistry Computer Center, University of Warsaw.

Table 1 Average properties of flexible chains (±standard error of simulation). $\varepsilon_g = 0$)

n	T^*	$\langle R_N^2 \rangle$	$\langle S_N^2 \rangle$	$\langle S^4 \rangle$	$\langle E_N \rangle$	$\langle f_t \rangle$
11	∞	74.95 ± 1.05	33.97 ± 0.53	1196	0.0000	0.378 ± 0.001
	5.0000	70.26 ± 1.01	32.09 ± 0.51	1071	0.910 ± 0.0006	0.366 ± 0.001
	3.3333	68.15 ± 0.92	31.21 ± 0.44	1015	0.1030 ± 0.0010	0.361 ± 0.002
	2.5000	65.61	30.16	950	0.1163	0.353
	2.0000	63.11	29.16	890	0.1314	0.347
	1.8182	61.33	28.44	845	0.1409	0.342
	1.6667	59.90	27.82	813	0.1502	0.338
	1.5385	58.31	27.16	775	0.1595	0.333
	1.4286	56.50	26.25	725	0.1724	0.330
	1.2500	33.99 ± 0.81	25.09 ± 0.32	664	0.1906 ± 0.0031	0.322 ± 0.002
	1.1111	51.26 ± 0.82	23.79 ± 0.30	598	0.2124 ± 0.0031	0.314 ± 0.002
	1.0000	47.97 ± 0.76	22.43 ± 0.26	532	0.2348 ± 0.0034	0.306 ± 0.002
	0.8333	42.42 ± 0.61	20.07 ± 0.19	423	0.2776 ± 0.0038	0.293 ± 0.002
	0.6667	37.24 ± 0.25	17.48 ± 0.11	318	0.3329 ± 0.0042	0.283 ± 0.001
	0.5000	31.75 ± 0.18	14.57 ± 0.08	216	0.4060 ± 0.0039	0.283 ± 0.001
24	∞	192.5 ± 1.2	86.94 ± 0.42	7916	0.0000	0.375 ± 0.001
	5.0000	178.6 ± 2.1	78.68 ± 0.67	6513	0.0925 ± 0.0007	0.363 ± 0.001
	3.3333	168.7 ± 1.0	75.37 ± 0.54	6012	0.1080 ± 0.0011	0.357 ± 0.002
	2.5000	159.0 ± 1.2	70.86 ± 0.48	5332	0.1280 ± 0.0013	0.351 ± 0.001
	2.0000	145.1 ± 1.9	65.05 ± 0.73	4525	0.1524 ± 0.0015	0.343 ± 0.001
	1.8182	137.0 ± 0.9	61.94 ± 0.41	4112	0.1684 ± 0.0012	0.339 ± 0.002
	1.6667	130.4 ± 1.3	59.13 ± 0.51	3755	0.1842 ± 0.0017	0.335 ± 0.002
	1.5385	121.4 ± 1.0	54.85 ± 0.52	3241	0.2038 ± 0.0022	0.331 ± 0.003
	1.4286	115.6 ± 1.8	52.86 ± 0.62	3012	0.2201 ± 0.0029	0.328 ± 0.002
	1.2500	102.0 ± 1.3	46.73 ± 0.53	2367	0.2601 ± 0.0032	0.320 ± 0.002
	1.1111	92.21 ± 0.93	41.08 ± 0.62	1825	0.3010 ± 0.0032	0.314 ± 0.003
	1.0000	81.78 ± 1.04	35.58 ± 0.55	1344	0.3453 ± 0.0033	0.309 ± 0.003
	0.8333	68.74 ± 0.81	30.06 ± 0.31	937	0.4050 ± 0.0029	0.303 ± 0.002
	0.6667	56.08 ± 0.85	25.68 ± 0.26	670	0.4696 ± 0.0030	0.301 ± 0.003
49	∞	462.4 ± 3.5	197.9 ± 1.9	41 344	0.0000	0.373 ± 0.001
	5.0000	425.5	182.5	35 472	0.0900	0.363
	3.3333	395.4	168.8	30 355	0.1087	0.356
	2.5000	347.5	150.1	24 231	0.1363	0.350
	2.0000	309.1	133.9	19 524	0.1674	0.343
	1.8182	291.2	122.5	16 361	0.1889	0.340
	1.6667	27.3	111.9	13 802	0.2125	0.335
	1.5385	234.5 ± 3.1	99.23 ± 2.42	10 838	0.2442 ± 0.0031	0.331 ± 0.002
	1.4286	215.6 ± 6.2	89.68 ± 2.63	8957	0.2700 ± 0.0028	0.327 ± 0.002
	1.2500	165.9 ± 4.3	68.86 ± 2.15	5175	0.3413 ± 0.0035	0.322 ± 0.002
	1.1111	135.5	54.65	3120	0.4050	0.319
	1.0000	118.8	49.61	2564	0.4443	0.315
	0.8333	115.9	41.95	1783	0.5111	0.310
	0.6667	84.13 ± 2.60	39.13 ± 1.11	1539	0.5585 ± 0.0021	0.300 ± 0.002
99	∞	1084 ± 6	450.0 ± 2.8	212 896	0.0000	0.371 ± 0.002
	5.000	885.1 ± 6.2	380.3 ± 3.6	152 264	0.0925 ± 0.0023	0.362 ± 0.001
	3.3333	773.4	334.4	120 171	0.1130	0.356
	2.5000	744.4	307.7	101 196	0.1385	0.350
	2.0000	634.9	278.5	87 624	0.1744	0.342
	1.6667	494.1 ± 4.2	202.3 ± 1.9	45 672	0.2405 ± 0.0018	0.335 ± 0.001
	1.4286	296.1 ± 2.3	116.3 ± 1.1	14 666	0.3451 ± 0.0031	0.329 ± 0.003
	1.2500	232.5 ± 3.2	91.07 ± 1.36	8664	0.4255 ± 0.0025	0.325 ± 0.002
	1.1111	181.7	72.32	5282	0.4973	0.324
	1.0000	148.3	69.74	4897	0.5315	0.318
	0.8333	141.1	63.22	4009	0.5861	0.310
	0.6667	121.0 ± 2.1	57.75 ± 0.95	3346	0.6501 ± 0.0018	0.313 ± 0.002
	∞	2486 ± 11	1041 ± 5	1 173 721	0.0000	0.372 ± 0.002
	5.0000	1938 ± 14	870.6 ± 3.6	793 595	0.0890 ± 0.0019	0.361 ± 0.002

Table 1 *continued*

n	T^*	$\langle R_N^2\rangle$	$\langle S_N^2\rangle$	$\langle S^4\rangle$	$\langle E_N\rangle$	$\langle f_t\rangle$
199	3.3333	1897	817.7	693044	0.1077	0.356
	2.5000	1350	582.1	354844	0.1420	0.348
	2.0000	1167	474.6	245399	0.1860	0.341
	1.8182	874.6±8.9	381.1±5.5	156501	0.2247±0.0047	0.338±0.002
	1.6667	757.4±9.3	286.2±4.8	91624	0.2780±0.0061	0.335±0.003
	1.5385	499.2±8.6	195.8±6.1	41393	0.3489±0.0042	0.332±0.003
	1.4286	454.0	163.8	28137	0.3974	0.328
	1.2500	263.7	121.9	15004	0.4959	0.327
	1.1111	204.2	109.0	11924	0.5569	0.325
	0.8333	184.6±5.1	88.16±2.11	7776	0.7069±0.0043	0.323±0.001
	0.6667	178.7±4.2	83.97±1.90	7051	0.7452±0.0051	0.316±0.002

Table 2 Exponents γ (equations (1a) and (1b)) calculated by various means

Reference	γ_R linear	γ_R star	γ_S linear	γ_S star
This work		1.211 ±0.004		1.178 ±0.005
16, 17[a]	1.184 ±0.002		1.186 ±0.004	
7[b]		1.184		1.1752
18[c]	1.176 ±0.0015		1.176 ±0.0015	
19[d]	1.1802		1.1832	

[a] Dynamic Monte Carlo, tetrahedral lattice

[b] Monte Carlo, face-centred lattice, dimerization technique

[c] Renormalization group theory

[d] Monte Carlo, tetrahedral lattice, pivot algorithm

Flexible chains

For the flexible chain model there are only two input parameters: the reduced temperature T^* and the chain length. In *Table 1* some output parameters are presented for chain lengths over a wide range of temperature. These parameters are $\langle R_N^2\rangle$, $\langle S_N^2\rangle$, $\langle f_t\rangle$ and the normalized mean energy $\langle E_N\rangle = E_{\text{conf}}T^*/(N+1)$. The normalized energy can be comparable for all systems under consideration and, moreover, it represents the mean number of energetic contacts for flexible chains (the second term in equation (2) disappears for flexible chains).

The values of $\langle S_N^2\rangle$ and $\langle R_N^2\rangle$ for the case of good solvent conditions (athermal chain) fulfil the scaling laws of equations (1a) and (1b). The values of both exponents γ_S and γ_R obtained from these equations are presented in *Table 2* together with other simulation results and theoretical predictions (with results concerning linear chains for comparison). It should be pointed out that our DMC simulation results obey power laws (1a) and (1b) with very good accordance. The rejection of the data concerning the shortest chains ($n = 11, 24$) does not change significantly the values of the exponents. Contrary to the renormalization group predictions, our $\gamma_S \neq \gamma_R$ and $\gamma_R > \gamma_S$ are similar to the data of Batoulis and Kremer[7] (Monte Carlo simulations on a different lattice using a different simulation method). This feature of scaling behaviour differs from that of linear chains where $\gamma_S \approx \gamma_R$ according to recent simulations[16,17,19]. This can be explained by the fact that the arms are too short to exhibit the correct scaling behaviour of $\langle R_N^2\rangle$.

Table 3 Parameters g (equation (2)) and g' (equation (12)) calculated by various means for the athermal chain

Reference	g	g'
This work[a]	0.590±0.005	1.183±0.008
1[b]	0.625	1.000
9[c]	0.667	1.166
7[d]	0.611	1.168
27, 28[e]	0.63	
5[f]	0.60±0.01	1.17±0.02
49[g]	0.633, 0.65	
This work (amplitude ratios)[h]	0.594±0.006	1.158±0.012

[a] Data extrapolated to infinite N

[b] Random walk model

[c] Renormalization group theory

[d] Monte Carlo, face-centred lattice, dimerization technique

[e] Monte Carlo, tetrahedral lattice

[f] Monte Carlo, simple cubic lattice

[g] Experimental, polystyrenes and polyisoprenes, respectively

[h] Amplitude ratio B_{br}/B_l. B_{br} was determined assuming parameter $\gamma = 1.186$ (the same as for linear chains)

The ratio $\langle S_N^2\rangle/\langle R_N^2\rangle$ changes with the length of an arm: from 0.453±0.008 for $N = 44$ to 0.419±0.004 for $N = 796$. These data are located between two theoretical limit predictions: $2^{1/2}/6$ $(=0.236)$ for the random flight star-branched polymer and 3/5 for the homogeneously filled hard sphere[14]. The next parameter describing the shape of a macromolecule is the reduced fourth moment:

$$\sigma_S(4, 2) = \langle S^4\rangle/\langle S^2\rangle^2 \tag{10}$$

The reduced fourth moment extrapolated (in the limit of $N = \infty$) has the value $\sigma_S = 1.10$. The random flight model predicts:

$$\sigma_S(4, 2) = \frac{120 - 120/f + 4/f^2}{15(3 - 2/f)^2} = 1.123 \tag{11}$$

The size of an arm of a star-branched polymer is usually compared with a linear chain of the same length and described by the following parameter:

$$g' = \langle R_N^2\rangle_{\text{br}}/\langle R_N^2\rangle_l \tag{12}$$

The parameters g (according to equation (2)) and g' were calculated using the data of Kolinski *et al.*[16,17] concerning linear chains on the same lattice with a similar number of segments and obtained by similar DMC simulations. The values of g and g' are presented in *Table 3* with other simulation results and theoretical predictions. Our results are obtained from the extrapolation in the limit of the

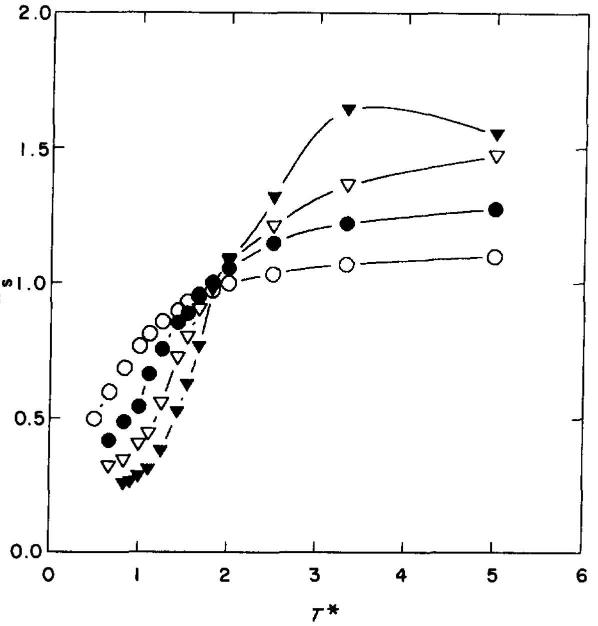

Figure 2 Expansion factor α_S^2 *versus* reduced temperature T^* for various lengths of flexible chain: ○, $N=44$; ●, $N=96$; ▽, $N=196$; ▼, $N=396$

infinite chain. In the random walk model we have the Zimm–Stockmayer formula (equation (2)), and using the renormalization group method of Miyake and Freed[9]:

$$g=\frac{3f-2}{f^2}\left\{1-\frac{4-d}{8}\left[\frac{13(f-1)(f-2)}{2(3f-2)}-\frac{4(f-1)(3f-5\ln 2)}{3f-2}\right]\right\} \tag{13}$$

where $d=3$ is the dimension of space. Parameter $g'=1$ for the random flight chain, and in Miyake–Freed theory is given by:

$$g'=1+\tfrac{1}{8}(f-1)(\ln 2-1/4)(4-d) \tag{14}$$

The results obtained in the our DMC simulation and in other simulations with different techniques and on different lattices[5,7,9,27,28] (*Table 3*) are in good agreement with these theoretical predictions. This agreement confirms that parameters g and g' are not sensitive to solvent quality, at least in the case of small functionality and in good solvent conditions.

In order to determine the location of the Θ temperature, we analysed the expansion factor of a polymer chain defined as:

$$\alpha_S^2=\langle S_N^2\rangle_{\mathrm{br}}/\langle S_N^2\rangle_0 \tag{15}$$

where $\langle S_N^2\rangle_0$ is the mean-square radius of gyration calculated for the rotational isomeric states model of star-branched polymer with the same number of segments and branches according to the following expression[15,34–39]:

$$\langle S_N^2\rangle_0=\frac{l^2}{N^2}\left\{fn\left[1+\frac{(n+4)(n-1)}{6}\right]+m^2\frac{m-1}{2}f(f-1)\right\}\frac{1+\langle\cos\mu\rangle}{1-\langle\cos\mu\rangle} \tag{16}$$

where μ is the valence angle. In the case of a tetrahedral lattice $\langle\cos\mu\rangle=1/3$. The results are presented in *Figure 2* where the expansion factor α_S^2 is plotted *versus* the reduced temperature for various chain lengths. The Θ temperatures can be found from *Figure 2* as points where $\alpha_S^2=1$; they increase with increasing chain length. All curves cross at approximately the same temperature $k\Theta/\varepsilon_g=1.88$. The Θ temperatures for the flexible linear chains were found to be between 2.12 (Monte Carlo simulations of Kolinski *et al.*[16,17]) and 2.25 ± 0.05 (Monte Carlo simulations of Kremer *et al.*[20]).

Below the Θ temperature a flexible star polymer collapses to a dense globule. This can be seen from *Figure 3* where the mean-square radius of gyration $\langle S_N^2\rangle$ is plotted *versus* the reduced temperature T^* for various chain lengths. The size of the chain diminishes continuously with decreasing temperature. Thus, it is impossible to estimate the location of the temperature of the collapse transition T_C from this figure. A crude estimate of the values of T_C can be made from *Figure 4* where the reduced heat capacity $C_V/k_BN\xi^2$ is plotted

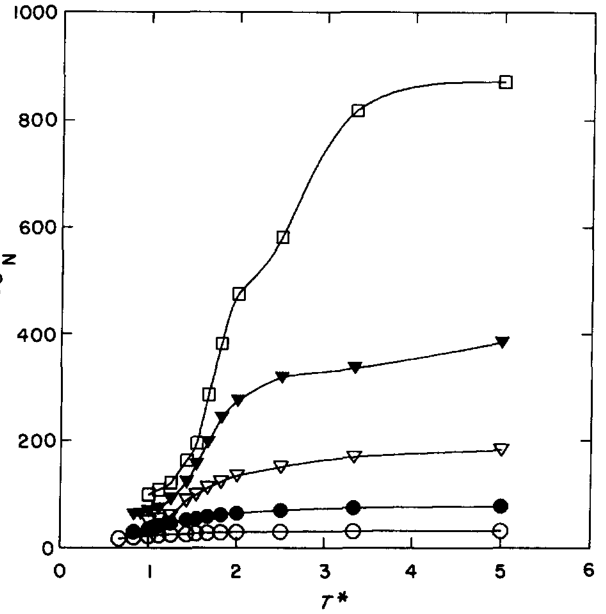

Figure 3 Mean-square radius of gyration $\langle S_N^2\rangle$ *versus* reduced temperature T^* for various lengths of flexible chain: ○, $N=44$; ●, $N=96$; ▽, $N=196$; ▼, $N=396$; □, $N=796$

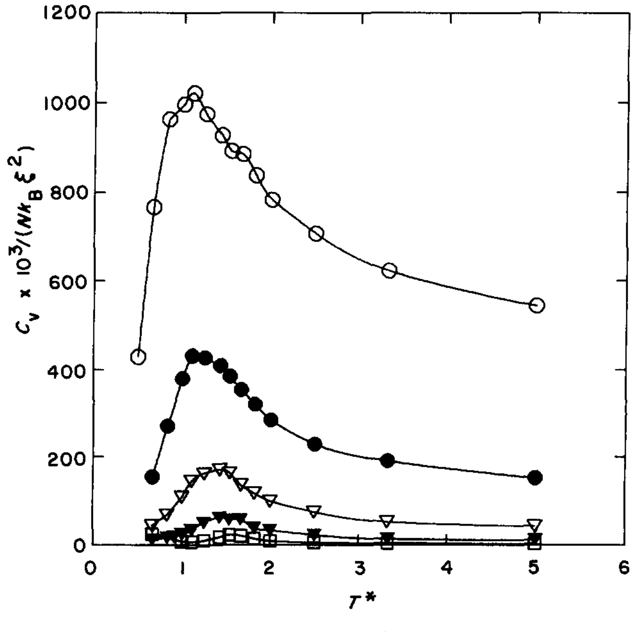

Figure 4 Reduced heat capacity $C_v/k_BN\xi^2$ *versus* reduced temperature T^* for various lengths of flexible chain. Symbols as in *Figure 3*

Table 4 Average properties of semiflexible chains

n	$\varepsilon_g/\varepsilon_a$	T^*	$\langle R_N^2\rangle$	$\langle S_N^2\rangle$	$\langle E_N\rangle$	$\langle f_t\rangle$
24	1	5.0000	197.3±2.8	86.37±1.14	0.4575±0.0051	0.408±0.002
		2.5000	189.0±3.2	82.89±1.44	0.4090±0.0064	0.438±0.002
		2.0000	184.0	80.36	0.3810	0.453
		1.6667	176.2	73.75	0.3467	0.467
		1.4286	167.0±2.3	71.45±1.26	0.3097±0.0045	0.481±0.002
		1.2500	157.1±2.0	65.24±1.25	0.2626±0.0051	0.496±0.003
		1.1111	139.5±2.2	56.09±1.33	0.2093±0.0074	0.507±0.003
		0.8333	91.04±1.16	38.31±1.01	−0.0253±0.0052	0.597±0.003
		0.6667	42.05±1.22	34.53±0.87	−0.2077±0.0027	0.700±0.002
24	2	2.0000	215.4	93.93	0.4446	0.471
		1.0000	254.1	102.8	0.3491	0.571
		0.6667	314.6±3.2	112.7±1.2	0.2367±0.0032	0.675±0.004
		0.5556	362.7±3.7	103.6±1.3	0.1168±0.0041	0.748±0.008
		0.5000	764.1	110.8	−0.0651	0.874
		0.4545	846.6±5.6	111.7±1.8	−0.0930±0.0027	0.897±0.008
		0.4167	856.6±7.3	112.6±2.3	−0.1035±0.0031	0.901±0.007
		0.3846	914.5±4.5	107.3±1.9	−0.1263±0.0022	0.914±0.004
24	3	1.6667	229.9	99.43	0.4375	0.496
		1.1111	268.7	110.5	0.3808	0.561
		0.8333	307.6	121.3	0.3233	0.624
		0.6667	366.0±4.1	137.4±2.5	0.2667±0.0051	0.686±0.004
		0.5556	447.0±3.8	160.7±2.2	0.2016±0.0059	0.747±0.005
		0.4762	576.2	186.6	0.1307	0.814
		0.4167	753.7	189.8	0.0472	0.878
		0	602.4	102.1	−0.0265	0.904
		0.3704	394.1	101.1	−0.0425	0.927
		0.3333	362.5±2.8	101.1±0.9	−0.0575±0.0018	0.933±0.002
100	1	5.0000	959.6	418.6	0.5035	0.403
		2.5000	864.8	369.9	0.4445	0.436
		2.0000	779.0±7.3	327.3±2.1	0.4018±0.0071	0.451±0.003
		1.6667	529.5	207.7	0.3158	0.465
		1.4286	334.9	133.0	0.2039	0.480
		1.2500	240.7±4.1	89.94±1.63	0.0733±0.0044	0.504±0.003
		1.1111	193.9±3.5	79.38±1.28	−0.0073±0.0035	0.524±0.004
		0.8333	170.1±3.8	77.23±1.06	−0.3264±0.0039	0.680±0.003
		0.6667	130.1	73.01	−0.4041	0.728
		0.5000	146.8	71.64	−0.4475	0.744
		0.4000	147.9	71.76	−0.4564	0.753
100	2	2.0000	1060	435.5	0.4854	0.468
		1.0000	965.9±5.1	405.9±2.3	0.3736±0.0071	0.568±0.004
		0.8333	729.8±8.2	284.6±2.8	0.3081±0.0052	0.608±0.003
		0.7143	437.4±4.9	168.0±1.7	0.1767±0.0036	0.663±0.003
		0.6667	576.6	180.6	−0.0792	0.809
200	2	2.5000	2067	911.9	0.4914	0.468
		1.0000	1499	581.7	0.3661	0.569
		0.8333	1527	542.7	0.3083	0.608
		0.7615	865.6±6.3	258.6±2.4	0.2080±0.0051	0.702±0.004
		0.7143	427.9±5.7	166.7±2.1	−0.0427±0.0065	0.760±0.003
		0.6667	554.7	194.0	−0.1261	0.814
		0.5000	411.4	177.9	−0.1863	0.845
200	3	1.6667	1915	852.0	0.1397	0.492
		1.1111	1828	858.7	0.1584	0.556
		0.8333	2295	1075	0.3561	0.621
		0.6667	2261±12	900.9±4.5	0.2859±0.0037	0.685±0.004
		0.5556	1712±9	643.3±3.1	0.0274±0.0022	0.803±0.005
		0.4762	872.4±8.5	379.8±2.4	−0.0928±0.0029	0.889±0.005
		0.4167	853.4	371.0	−0.1201	0.902

Table 4 *continued*

n	$\varepsilon_g/\varepsilon_a$	T^*	$\langle R_N^2\rangle$	$\langle S_N^2\rangle$	$\langle E_N\rangle$	$\langle f_t\rangle$
		0.3704	809.1	363.7	−0.1231	0.907
200	3.5	2.0408	2418	1045	0.5069	0.471
		0.9524	2265	969.2	0.3890	0.592
		0.8163	2442	1131	0.3533	0.629
		0.6645	2944	1273	0.2957	0.688
		0.5495	2840 ± 14	1282 ± 5	0.2282 ± 0.0081	0.751 ± 0.004
		0.4926	907.3 ± 8.6	393.0 ± 2.6	−0.0495 ± 0.0042	0.883 ± 0.005
		0.4082	1371	389.6	−0.0537	0.892
		0.3361	1258	371.27	−0.0618	0.894
200	4	2.0000	1996	930.3	0.5072	0.473
		1.0000	2167	880.9	0.4007	0.583
		0.6667	3566	1475	0.2975	0.689
		0.5556	3459	1361	0.2402	0.747
		0.5000	4384 ± 23	1646 ± 9	0.2033 ± 0.0064	0.781 ± 0.004
		0.4545	1931 ± 12	1057 ± 9	0.0748 ± 0.0038	0.844 ± 0.004
		0.4348	1550 ± 9	643.4 ± 4.2	0.0114 ± 0.0019	0.872 ± 0.003
		0.4167	2336	730.1	−0.0123	0.882
		0.3333	2730	702.7	−0.0242	0.893

versus the reduced temperature (according to the fluctuation theorem $C_V/k = \langle E^2\rangle - \langle E\rangle^2$; $\xi = \varepsilon_g/k_B T$). The collapse temperature T_C can be estimated with about 10% accuracy from the location of a peak on the C_V curves which are sharper for the shortest chains. $T_C = 1.00$, 1.16, 1.4, 1.5 and 1.6 for $N = 44$, 96, 196, 396 and 796, respectively. Consequently one may expect that for $N \to \infty$, T_C and Θ coincide. The dimensions of the collapsed chain undergo scaling laws: $\langle R_N^2\rangle = 3.88\,(N-1)^{0.542 \pm 0.004}$ and $\langle S_N^2\rangle = 1.86\,(N-1)^{0.548 \pm 0.008}$, at the temperature $T^* = 0.667$. The values of these exponents are lower than the value of 2/3 predicted by de Gennes[14]. Simulations of linear chains and other models of branched polymers also give low values of the exponents ($\gamma = 0.55$ for linear chains[16,17] and 0.55 for a star with $f = 6$ arms[34–39]). This is caused by finite chain effects. The reduced moments of collapsed chains of all lengths, $\sigma_S(4, 2) = 1$, indicate that in practice the collapsed star polymers occur in one conformation. Parameter $g = 1.00$ (at the temperature $T^* = 1.0$), which means that the distribution of segments is the same as in the collapsed linear chains. There is no ordering in the collapsed structures — the mean fraction of *trans* states $\langle f_t\rangle$ decreases slowly and smoothly with decreasing temperature (f_t is about 0.37 in the case of the athermal model) and below the transition reaches values close to 0.3 (*Figure 5*).

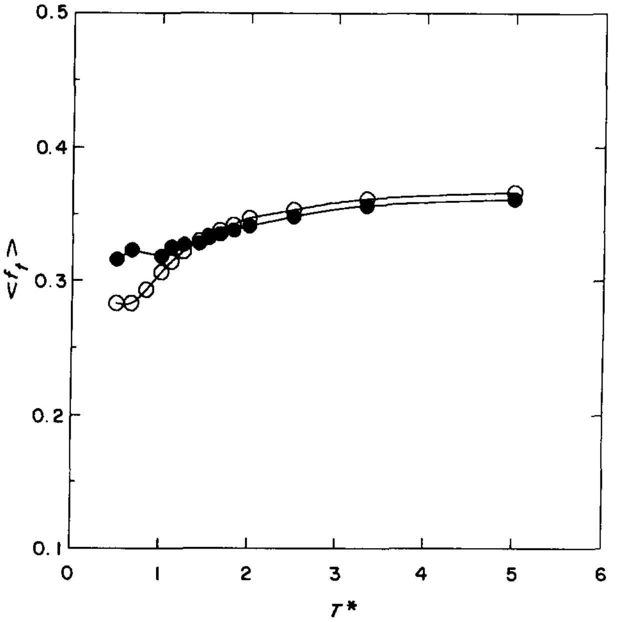

Figure 5 Mean fraction of *trans* states $\langle f_t\rangle$ *versus* reduced temperature T^* for the case of flexible chains: ○, $N = 44$; ●, $N = 96$

Semiflexible chains

Table 4 summarizes data concerning semiflexible polymer chains (with local stiffness $\varepsilon_g \neq 0$). The ratio $\varepsilon_g/\varepsilon_a$ becomes an additional input parameter. All output parameters remain the same as in the case of flexible star polymers. The example of the behaviour of the mean-square radius of gyration $\langle S_N^2\rangle$ *versus* the reduced temperature T^* is presented in *Figure 6* for the total number of segments $N = 96$ for various values of the ratio $\varepsilon_g/\varepsilon_a$. In order to estimate the location of the Θ temperature we plotted in *Figure 6* values of $\langle S_N^2\rangle$ calculated for a random flight chain with the same local interactions (RIS model). The detailed derivation of the formula for this S_0^2 is presented in the papers of Mattice *et al.*[54,55]. An intersection of the RIS curve with a curve obtained from simulations gives the location of the Θ temperature with an accuracy of about ±0.05. For the case of a star polymer with arm length $n = 24$, the Θ temperature is equal to 1.80, 1.02 and 0.82 for the ratio $\varepsilon_g/\varepsilon_a = 1$, 2 and 3, respectively (1.80, 2.04 and 2.46 in $k_B T/\varepsilon_a$ units). For the longest chain ($N = 796$) the Θ temperature is equal to 1.00, 0.82 and 0.51 for the ratio $\varepsilon_g/\varepsilon_a = 3$, 3.5 and 4, respectively (3.00, 2.87 and 2.04 in $k_B T/\varepsilon_a$ units).

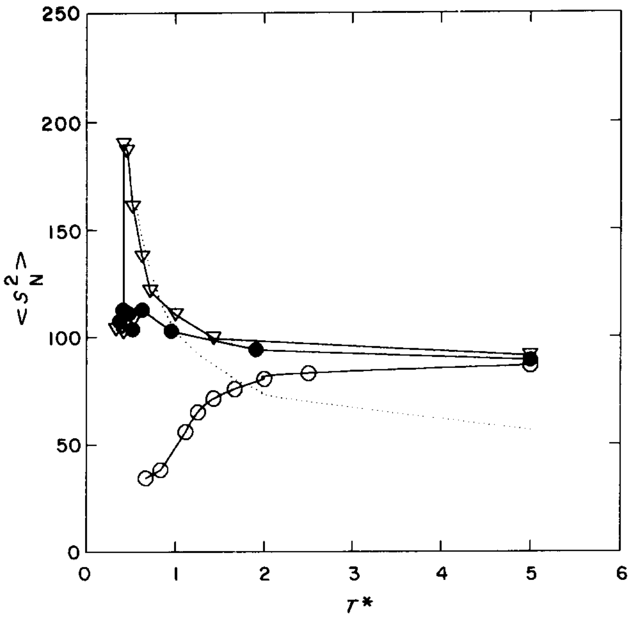

Figure 6 Mean-square radius of gyration $\langle S^2_N \rangle$ *versus* reduced temperature T^* for the case of semiflexible chain of total length $N=96$ and for various $\varepsilon_g/\varepsilon_a$ ratios: ○, 1; ●, 2; ▽, 3. The dotted curve represents results of the RIS model

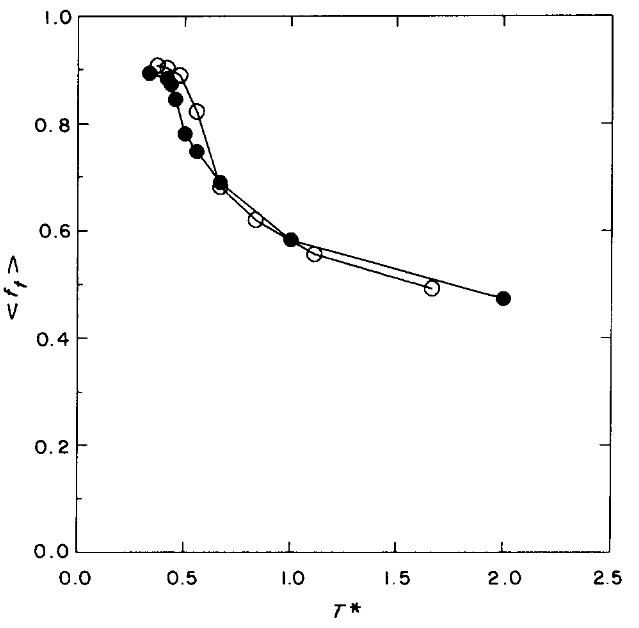

Figure 7 Mean fraction of *trans* states $\langle f_t \rangle$ *versus* reduced temperature T^* for the case of semiflexible chain of total length $N=796$ and for $\varepsilon_g/\varepsilon_a=3$ (○) and 4(●)

It can be seen from *Figure 6* that semiflexible chains undergo the collapse transition to a dense state, similar to the flexible chains, for short as well as for long chains. But this transition takes two distinct forms: chains with low values of the ratio $\varepsilon_g/\varepsilon_a$ ($=1$ or 2) undergo smooth collapse transitions similar to those of flexible chains, while chains with higher $\varepsilon_g/\varepsilon_a$ ratios (>3) undergo a very sharp transition. In the first case, long-distance attractive interactions override local stiffness. Even at the intermediate temperatures, the radius of gyration does not increase significantly; at low temperatures it decreases smoothly. In the second case the behaviour of star polymers at intermediate temperatures is similar to that of more flexible chains but at lower temperatures the size of a macromolecule increases and then sharply decreases. This means that local interactions prevail and a collapsed state is a dense highly ordered structure. The size of these globules is considerably greater than those of flexible chains and semiflexible chains with low $\varepsilon_g/\varepsilon_a$ ratios. It can be seen from *Table 4* that at higher temperatures the values of f_t are close to those of the RIS model, then change sharply reaching values between 0.9 and 1.0 for the collapsed structures, independent of the length of the chain. Examples of the courses of f_t *versus* T^* are presented in *Figure 7*. Plots of the reduced heat capacity $C_V/k_B N\xi^2$ *versus* temperature T^* for all chain lengths under consideration are presented in *Figure 8*. The location of the sharp peak on C_V curves and the jump in S^2 (or C_V, f_t and E_N) *versus* T^* curves can be treated as a crude estimation of the collapse temperature T_C. In the case of $N=44$, T_C is 0.42 for $\varepsilon_g/\varepsilon_a=3$. For the longest chain ($N=796$), values of T_C are 0.55, 0.48 and 0.44 for $\varepsilon_g/\varepsilon_a=3$, 3.5 and 4, respectively (1.65, 1.68 and 1.76 in $k_B T/\varepsilon_a$ units).

Examples of collapsed structures are presented in *Figures 9a* and *b*. Flexible chain seems to be a random dense globule (*Figure 9a*). In the case of stiff chains (*Figure 9b*) one can see folded domains of almost pure *trans* states. The structure is not unique: in every simulation run a slightly different collapsed structure was obtained: all output parameters are close but the number and length of ordered stretches varies. This feature is similar to the case of linear chains[16,17].

CONCLUSIONS

The dynamic Monte Carlo simulations of a tetrahedral lattice model of uniform star-branched polymers were concentrated on the collapse transition. Some static properties of star macromolecules under various conditions were calculated. These data (the mean-square radius of gyration, the mean-square centre-to-end distance, fraction of *trans* states) in good solvent

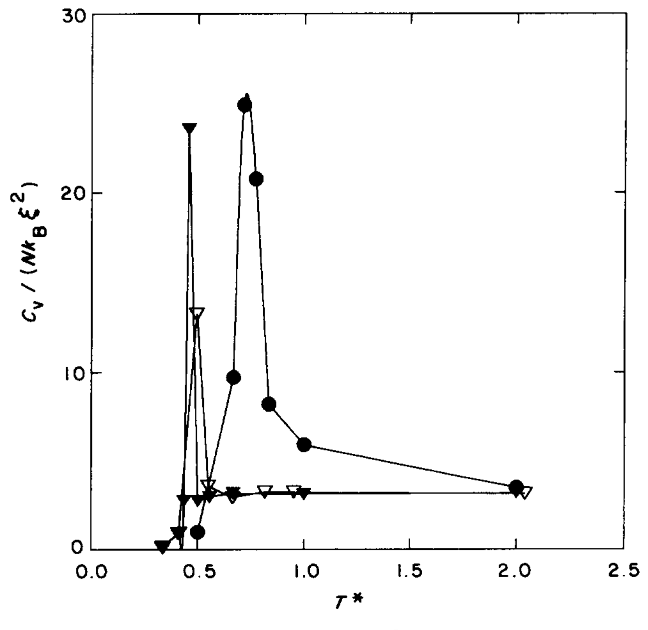

Figure 8 Reduced heat capacity $C_v/k_B N\xi^2$ *versus* reduced temperature T^* for the case of semiflexible chain of total length $N=796$ and for $\varepsilon_g/\varepsilon_a=2$ (●), 3.5 (▽) and 4(▼)

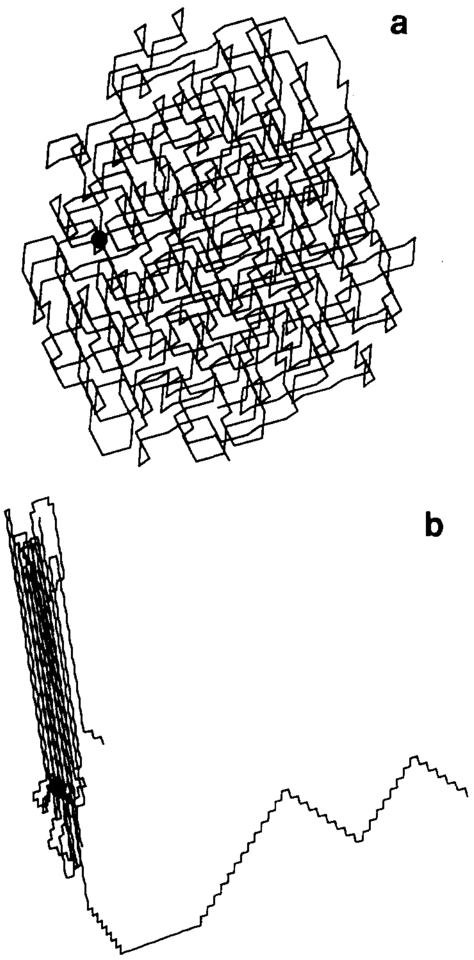

Figure 9 Example of conformation of (a) collapsed flexible chain of total length $N=796$ at $T^*=0.6667$ and (b) collapsed semiflexible chain of length $N=796$, $\varepsilon_g/\varepsilon_a=4$, at $T^*=0.3333$. ●, branching point

conditions (high temperature, random coil state) exhibit behaviour which is very close to that of linear chains and other star-branched polymer models. The size parameters scale according to well known scaling laws and the parameter g is close to the value of the random flight model in the whole region above the Θ temperature. The behaviour of a star polymer with decreasing temperature (deterioration of the solvent) depends on the local interactions of the chain. In the case of flexible chains (with no local stiffness) the size of a polymer chain and the total configurational energy decrease smoothly and the fraction of *trans* states decreases smoothly and very slowly. In the case of semiflexible chains (with local stiffness) the behaviour of the polymer is similar for low $\varepsilon_g/\varepsilon_a$ ratios only. For higher ratios the size of a chain increases and then sharply decreases. The fraction of *trans* states increases sharply in semiflexible chains for all $\varepsilon_g/\varepsilon_a$ ratios. At the Θ temperature, where repulsive interactions are balanced with attractions, the polymer coil scales as the random flight model. The location of the Θ temperature (1.88) is different from that of linear chains on the same lattice (2.12)[16,17]. The expansion factor of a star polymer changes very smoothly with temperature. Its courses on the plot are almost identical to those of linear chains for all chain lengths under consideration. In the case of semiflexible chains, the Θ temperature becomes lower with increasing $\varepsilon_g/\varepsilon_a$ ratio in a similar region as for linear polymers[16,17]. Generally $\Theta_{br} < \Theta_l$ for both flexible and semiflexible chains. The same behaviour was recently predicted by the analytical theory[21].

Further decrease of the temperature leads to the collapse transition of a star macromolecule. There are two different kinds of transitions: a smooth (continuous) transition in the case of flexible chains and semiflexible chains with low $\varepsilon_g/\varepsilon_a$ ratios; and a sharp (discontinuous) transition in the case of semiflexible chains with higher values of $\varepsilon_g/\varepsilon_a$ ratio. The location of the transition temperature T_C depends on the length of a chain and on the $\varepsilon_g/\varepsilon_a$ ratio. In the case of flexible chains, $T_C=1.6$ for the longest polymer ($N=796$). A simple extrapolation to the infinite chain leads to the value of $T_C=1.8$, which is very close to the Θ temperature. In the case of semiflexible chains, T_C decreases with increasing values of the $\varepsilon_g/\varepsilon_a$ ratio ($N=796$): from 0.48 (2) to 0.44 (4). These values are slightly lower compared with those of linear chains[16,17] ($N=400$): 0.57 (3) and 0.50 (4). Generally, the transition temperature decreases with the stiffness of the polymer chain.

The strength of the local stiffness assigns polymers to one of two distinct classes. Flexible chains collapse to dense globules. Semiflexible chains collapse to highly ordered (but not unique) structures consisting of stretches of *trans* states with the minimum number of bends.

ACKNOWLEDGEMENTS

This research was partially supported by grant no. 12-500/4/BW-322. Stimulating discussions with Dr Andrzej Kolinski are gratefully acknowledged.

REFERENCES

1 Zimm, B. H. and Stockmayer, W. H. *J. Chem. Phys.* 1949, **17**, 1301
2 Daoud, M. and Cotton, J. P. *J. Phys.* (*Paris*) 1982, **43**, 531
3 Birshtein, T. M. and Zhulina, E. B. *Polymer* 1984, **25**, 1453
4 Birshtein, T. M., Zhulina, E. B. and Borisov, O. V. *Polymer* 1986, **27**, 1078
5 Whittington, S. G., Lipson, J. E. G., Wilkinson, M. K. and Gaunt, D. S. *Macromolecules* 1986, **19**, 1241
6 Grest, G. S., Kremer, K. and Witten, T. A. *Macromolecules* 1987, **20**, 1376
7 Batoulis, J. and Kremer, K. *Macromolecules* 1989, **22**, 4277
8 Rey, A., Freire, J. J. and Garcia de la Torre, J. *J. Chem. Phys.* 1989, **90**, 2035
9 Miyake, A. and Freed, K. F. *Macromolecules* 1983, **16**, 1228
10 Grest, S. G., Kremer, K., Milner, S. T. and Witten, T. A. *Macromolecules* 1989, **22**, 1904
11 Sikorski, A. *Makromol. Chem.* in press
12 Baumgartner, A. in 'Monte Carlo Methods in Statistical Physics' (Ed. K. Binder), Springer, Berlin, 1984, Ch. 4
13 Yamakawa, H. 'Modern Theory of Polymer Solution', Harper and Row, New York, 1971
14 de Gennes, P. G. 'Scaling Concepts in Polymer Physics', Cornell University Press, Ithaca, 1979
15 Flory, P. J. 'Principles of Polymer Chemistry', Cornell University Press, Ithaca, 1953
16 Kolinski, A., Skolnick, J. and Yaris, R. *J. Chem. Phys.* 1986, **85**, 35
17 Kolinski, A., Skolnick, J. and Yaris, R. *Macromolecules* 1987, **20**, 438
18 LeGuillou, J. C. and Zinn-Justin, J. *Phys. Rev. B* 1980, **21**, 3976
19 Zifferer, G. *Macromolecules* 1990, **23**, 3166
20 Kremer, K., Baumgartner, A. and Binder, K. *J. Phys. A: Math. Gen.* 1982, **15**, 2879
21 Ganazzoli, F. and Allegra, G. *Macromolecules* 1990, **22**, 262
22 Bruns, W. and Carl, W. *Macromolecules* 1991, **24**, 209
23 Huber, K., Buchard, W., Bangle, S. and Fetters, L. J. *Polymer* 1987, **28**, 1990; 1997
24 Bishop, M. and Clarke, J. H. R. *J. Chem. Phys.* 1989, **90**, 6647
25 Benoit, H. *J. Polym. Sci.* 1953, **9**, 507
26 Zimm, B. H. and Kilb, R. W. *J. Polym. Sci.* 1959, **37**, 19

27 Kolinski, A. and Sikorski, A. *J. Polym. Sci., Polym. Lett. Edn* 1982, **20**, 177
28 Kolinski, A. and Sikorski, A. *J. Polym. Sci., Polym. Chem. Edn* 1984, **20**, 3147
29 Sikorski, A. and Kolinski, A. *J. Polym. Sci., Polym. Chem. Edn* 1984, **22**, 97
30 Mazur, J. and McCrackin, F. *Macromolecules* 1977, **10**, 326
31 Barett, A. J. and Tremain, D. L. *Macromolecules* 1987, **20**, 1687
32 Mattice, W. L. *Macromolecules* 1980, **13**, 505
33 Croxton, C. A. *Macromolecules* 1988, **21**, 2269
34 Freire, J. J., Prats, R. and de la Torre, J. G. *Macromolecules* 1984, **17**, 1815
35 Freire, J. J., Pla, J. and Prats, R. *Macromolecules* 1986, **19**, 452
36 Freire, J. J., Rey, A. and de la Torre, J. G. *Macromolecules* 1986, **19**, 457
37 Rey, A., Freire, J. J. and de la Torre, J. G. *Macromolecules* 1987, **20**, 342
38 Rey, A., Freire, J. J. and de la Torre, J. G. *Macromolecules* 1987, **20**, 2385
39 Rey, A., Freire, J. J. and de la Torre, J. G. *Macromolecules* 1990, **23**, 3948
40 Smit, B., van der Put, A., Peters, C. J., de Swaan Arons, J. and Michels, J. P. J. *J. Chem. Phys.* 1988, **88**, 3372
41 Boothroyd, A. T. and Ball, R. C. *Macromolecules* 1990, **23**, 1729
42 McCrackin, F. L. and Mazur, J. *Macromolecules* 1981, **14**, 1214
43 Lipson, J. E. G., Gaunt, D. S., Wilkinson, M. K. and Whittington, S. G. *Macromolecules* 1987, **20**, 186
44 Murat, M. and Grest, S. G. *Macromolecules* 1989, **22**, 4054
45 Burchard, W. *Adv. Polym. Sci.* 1983, **48**, 1
46 Roovers, J. E. L. and Bywater, S. *Macromolecules* 1974, **7**, 443
47 Hadjichristidis, N. and Roovers, J. E. L. *J. Polym. Sci., Polym. Phys. Edn* 1974, **12**, 2521
48 Hadjichristidis, N. and Fetters, L. J. *Macromolecules* 1980, **13**, 191
49 Bauer, B. J., Hadjichristidis, N. and Fetters, L. J. *J. Am. Chem. Soc.* 1980, **102**, 2410
50 Huber, K., Burchard, W. and Fetters, L. J. *Macromolecules* 1984, **17**, 541
51 Khasat, N., Pennisi, R. W., Hadjichristidis, N. and Fetters, L. J. *Macromolecules* 1988, **21**, 1100
52 Skolnick, J. and Kolinski, A. *Ann. Rev. Phys. Chem.* 1989, **40**, 207
53 Carmesin, I. and Kremer, K. *Macromolecules* 1988, **21**, 2819
54 Mattice, W. L. *Macromolecules* 1976, **9**, 48
55 Mattice, W. L. and Carpenter, D. K. *Macromolecules* 1976, **9**, 53